Energy & Environmental Science

Accepted Manuscript

This article can be cited before page numbers have been issued, to do this please use: D. Massazza, R. Parra, J. P. Busalmen and H. E. Romeo, *Energy Environ. Sci.*, 2015, DOI: 10.1039/C5EE01498K.

ROYAL SOCIETY OF CHEMISTRY

www.rsc.org/ees

Energy and Environmental Science

Dynamic Article Links ►
View Article Online
DOI: 10.1039/C5EE01498K

Cite this: DOI: 10.1039/c0xx00000x

www.rsc.org/ materials

PAPER

New ceramic electrodes allow reaching the target current density in bioelectrochemical systems

Diego Massazza,[a] Rodrigo Parra,[b] Juan P Busalmen[a] and Hernán E Romeo[*,c]

Received (in XXX, XXX) Xth XXXXXXXXX 20XX, Accepted Xth XXXXXXXXX 20XX

DOI: 10.1039/b000000x

Whereas most of the studies conducted nowadays to boost electrode performance in bioelectrochemical systems (BES) are focused on carbonaceous scaffolds, in this study we demonstrate that ice-templated titanium-based ceramics (ITTC) can provide a new alternative for this purpose. We combined the chemistry of titanium suboxides (Ti_4O_7) with an ice-templating technique (ISISA) to produce electrically conducting and highly porous (88% porosity) 3D architectures. The ITTC platforms were characterized by strongly aligned macrochannels that provided a direct path for substrate supply under a flow-through configuration, while supporting the growth of electroactive *Geobacter sulfurreducens* biofilms. This new electrode material is demonstrated to outperform graphite when used as an anode in bioelectrochemical reactors, providing volumetric current densities of 9500 $A.m^{-3}$, equating to projected current densities of 128.7 $A.m^{-2}$ and maximum power densities of 1.9 $kW.m^{-3}$. The performance of the ITTC scaffolds levels that of any of the available materials on the current state of research. The presented alternative may lead to the start of a branch into the exploration of conducting ITTC materials in the growing area of bioelectrochemical technologies.

Introduction

Electrochemical processes that benefit from microbial biofilms as catalysts for electrode reactions have received increased attention during the past few years.[1,2] By virtue of recently discovered electro-active bacteria they now allow interconverting chemical energy and electricity with minor effort and low costs. Main technological developments in this area include energy recovery coupled to cleaning wastewater in microbial fuel cells (MFC) and, in the opposite direction, the production of commodity compounds in microbial electrosynthesis cells (MEC).[2]

The main drawback for successful entrance of these technologies into market is their low current density yield. It is now well recognized that current density produced by an electrochemically active biofilm is typically limited to 6-10 $A.m^{-2}$ in optimal laboratory conditions[3] and that the limit is determined by a physiological (respiratory) constrain on the bacterial population, which is derived from the imperfect conductivity of the biofilm matrix.[3-5] As soon as the biofilm thickness is greater than 50-60 µm, the progression of biofilm growth leads to the accumulation of idle cells in upper layers, which are impaired to contribute to current production.[6] In this context, actual efforts from materials science are directed to increase the effective electrode area as a mean for getting bioelectrodes with improved performance. The actual paradigm in this direction is the pursuit of porous materials with open aspects along which bacterial biofilms can be grown, at a rate limited only by biological factors.

An attractive way for producing porous bioelectrodes is that based on carbonization of natural materials. Porous 3D electrodes have been produced for example from kenaf stems[7] and pomelo peel[8] that were able to support projected current densities (PCD) of about 25 and 40 $A.m^{-2}$, respectively. Carbonization of a man-made product, corrugated cardboard, proved to be even better, yielding a PCD of about 70 $A.m^{-2}$ under a single layer configuration.[9] The key concept behind of these developments is taking advantage of already available 3D carbon configurations, but it is constrained to some extent to finding materials able of being carbonized with the appropriate structure. This is not the situation with materials synthesized *de novo* that can be conceptually designed according to specific needs. For example, electrodes bearing multidirectional pores in the range of tens of micrometers have been highlighted as valuable, because they can facilitate fluid flow.[10] This feature is found in electrospun carbon fibre mats, which exhibiting extremely low specific density allow efficient substrate supply for bacteria and promote the production of about 30 $A.m^{-2}$ of PCD.[11] Alternatively, unidirectional channels have also proved to be efficient in supporting bacterial growth at one of the highest levels, as shown by Katuri et al.[12] These authors built-up bioanodes via ice-segregation induced self-assembly (ISISA) on multiwall carbon nanotubes dispersed in a chitosan aqueous solution (MWCNT/CHI), leading to macroporous scaffolds with unique highly aligned macrochannels, which allowed increasing the bioelectrochemical performance. The material supported the growth of *G. sulfurreducens* biofilms generating 24.5 $A.m^{-2}$ of PCD, a value that clearly competes with that produced on carbonized materials.

On other branches of scientific research, and featuring low cost, biocompatibility and chemical stability, titanium oxides have gained a wide interest as building blocks for the design of porous structures. Whereas titanium dioxide (TiO_2), as a wide-band gap semiconductor, exhibits photocatalytic and photovoltaic properties;[13,14] its chemical reduction to electrically conducting titanium suboxides has proven to be specially attractive towards platforms with interesting magnetic and transport properties.[15,16] Titanium substoichiometric oxides of general formula Ti_nO_{2n-1} (with n between 4 and 10) are known as Magnéli phases[17] and

View Article Online
DOI: 10.1039/C5EE01498K

have been already used to prepare electrically conducting macroporous supports displaying uniform pore sizes (~2µm) and high porosity values (~60%), which makes them attractive for building up ceramic electrodes.[18]

In this context, and accounting for the need of producing *new electrode materials* for keeping on boosting microbial current densities in bioelectrochemical applications, in this study we demonstrate how the requirements identified as essential for bioelectrodes (high electrical conductivity, open porous structures and highly ordered porosity) can be obtained from ceramic materials to provide new alternatives in microbial electrocatalysis.

Herein, we report on the use of a cryogenic templating technique (ISISA) in combination with the chemistry of titanium suboxides (Magnéli phases) to build up new ice-templated titanium-based ceramics (ITTC) featuring biocompatibility towards *Geobacter sulfurreducens*, unidirectionally ordered macrochannels (10-15µm in diameter), maximized electrical conductivity and long term stability. The proposed ITTC electrodes challenge traditional carbon-based configurations in supporting the growth of electroactive bacterial films, with an energy conversion performance which levels that of any of the available materials on the current state of research.

Results and Discussion

In the way to produce ITTC electrodes, TiO_2 porous scaffolds with a precisely controlled architecture were firstly prepared by ISISA (see Experimental section). These scaffolds were pieces of about 1.5-2.0 x 1cm^2 (Fig. 1A) presenting a channelled pattern with an average channel size of 10-15 µm. The monoliths were ultra-lightweight, self-supported and presented bulk densities ranging between 0.500-0.635 g/cm^3 (85-88% porosity). Their most remarkable feature was the strongly anisotropic orientation of the pores (Fig. 1B). Pores were indeed interconnected, as evidenced by liquid penetration experiments.

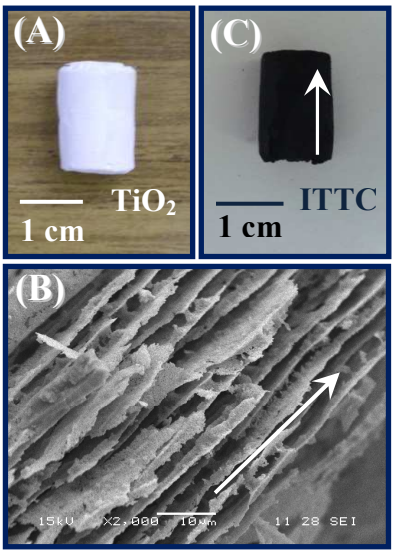

Fig. 1 (A) 3D TiO_2 porous scaffold, precursor of ITTC electrodes, **(B)** SEM image of the internal architecture of the TiO_2 scaffold, and **(C)** ITTC electrode obtained by reduction of TiO_2 porous scaffolds (for details, see Experimental section). Arrows indicate the freezing direction.

TiO_2 porous monoliths were reduced at high temperature in the presence of metallic zirconium under vacuum. After the reducing treatment, from which electrically conducting ITTC electrodes were finally obtained (see Experimental section and Figs.S1/S2), samples turned dark blue in color (Fig. 1C) as typically observed when oxygen vacancies are generated in a TiO_2 network.[19] It is interesting to note that ITTC electrodes kept both the same low bulk densities and scaffold integrity as those of the 3D TiO_2 precursor.

To evaluate the bioelectrochemical performance of the new electrodes, they were used as the working electrode in a continuous culture electrochemical reactor and polarized to 0.2 V (Ag/AgCl–3M NaCl). For promoting full colonization of the internal microstructure of the electrodes, the ITTC platforms were set in a flow-through configuration according to a previous report[12] (see Experimental section). As can be seen in Fig. 2, electricity-producing biofilms of *G. sulfurreducens* readily grew on ITTC electrodes reaching an unprecedented volumetric current density of almost 9500 A.m^{-3} after 200 h.

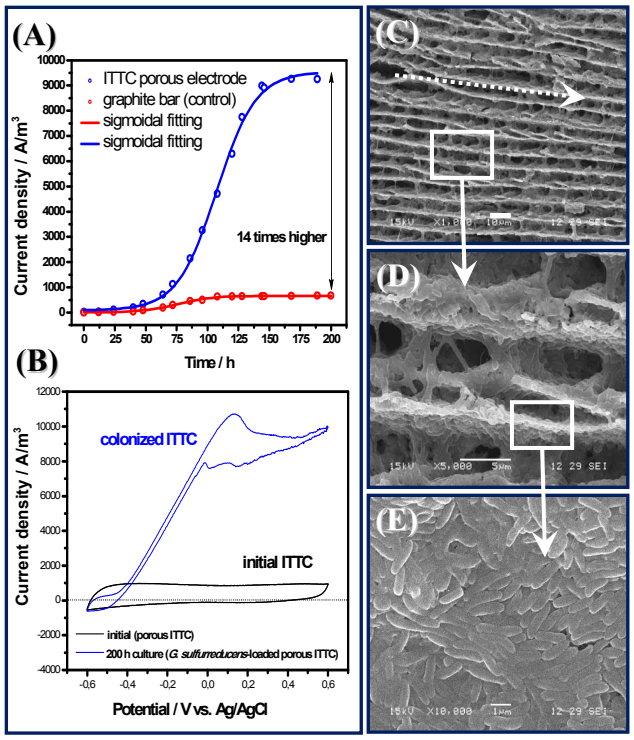

Fig. 2 (A) Chronoamperometry illustrating growth and electrocatalytic activity of *G. sulfurreducens* biofilms on ITTC macroporous electrodes, compared to a dense graphite bar; **(B)** Cyclic voltammograms recorded at a rate of 0.01 V.s^{-1} on macroporous ITTC, before (initial) and after (200 h) biofilm formation; **(C)** SEM of ITTC internal microstructure after current production (dotted arrow indicates porosity orientation); **(D)** biofilm adhered to the aligned porosity features; **(E)** magnification of the biofilm shown in **(D)**. Bars: (C) 10 µm, (D) 5 µm, and (E) 1 µm.

These results confirm not only the biocompatibility of ITTC electrodes towards *G. sulfurreducens*, but also that they can effectively act as electron acceptors for this bacterial strain with high efficiency. It is to note indeed that according to the results included in the Supplementary Material (Figs.S3/S4), biofilms grown on dense Ti_4O_7 electrodes (bars) were 7 times more

View Article Online
DOI: 10.1039/C5EE01498K

catalytic towards acetate electro-oxidation than those grown on standard graphite bars. This could be somehow related to the presence of a corundum-like crystallographic structure in Ti_4O_7 (the crystal structure of Ti_4O_7 is made up of rutile-type slabs separated by shear planes with a corundum-like atomic arrangement),[20] the same as that found in iron (III) oxides (α-Fe_2O_3 polymorph, the most common form of Fe_2O_3) that function as the natural electron acceptor for this bacterial strain.

It is worth mentioning that the volumetric current density obtained from the porous material was 14 times higher than that typically obtained for dense graphite bars (Fig. 2A). Interestingly, the value of PCD obtained on ITTC goes indeed well further than that claimed as the target to support the development of bioelectrochemical applications.[21] Expressing ITTC electrode performance as normalized to its projected surface area (128.7 $A.m^2$), allows the direct comparison with that from other materials and confirms that this new electrode can outcompete carbonaceous ones in the current state of research (Fig. 3). This high performance corresponds to a power density of 1.9 $kW.m^{-3}$, according to calculations made on the conservative position of Borole *et al.*,[21] which is assuming a voltage output of 0.2 V under load conditions. This power density is higher than that claimed as the target for sustainability of bioelectrochemical technologies.[21] It is worth mentioning that ITTC electrodes remained unaltered in the culture medium during the whole experimental lapse, sometimes extending for over a month. This reveals the robust electrode integrity (intrinsic to its ceramic nature), a feature that has been highlighted as an aspect of paramount importance in BES.

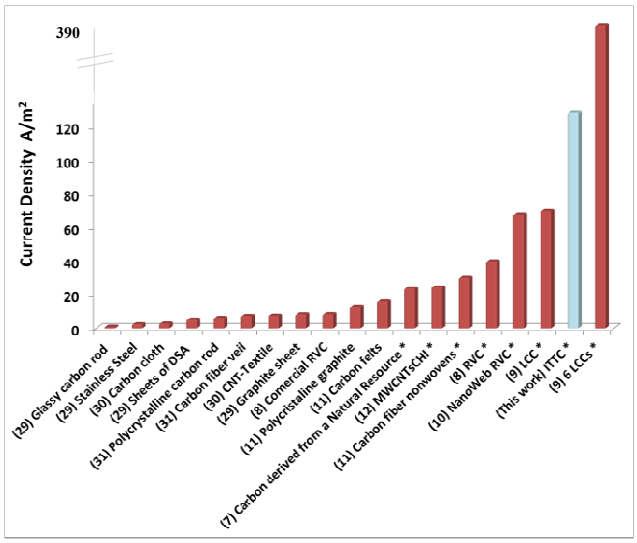

Fig. 3 Comparison of ITTC electrode performance with that of the current state-of-the-art electrodes. The asterisks indicate porous supports whose values are expressed as current density normalized to the projected surface area of the electrode. Although the experimental conditions are not exactly the same across all the compared electrodes, the current density values reported in each case correspond to the best electrode performance (that is, ensuring maximal current output from the bacterial population), so the comparison can be considered as a useful framework to put the ITTC electrode into context. The number in brackets indicates the corresponding reference.

Fig. 2B shows the voltammograms typically registered on ITTC electrodes before and after microbial colonization and growth (see also Fig.S5 in the Supplementary Material for cyclic voltammetry tests during biofilm evolution on ITTC, and Fig.S6 for comparison of cyclic voltammetries between ITTC and a typical graphite bar after biofilm formation). In the presence of a biofilm, the obtained turnover signature was indicative of the catalytic oxidation of acetate by metabolically active *G. sulfurreducens* cells and displayed a half-wave potential of about -0.25 V. The response is quiet similar to that obtained from biofilms of *G. sulfurreducens* grown on other electrode materials as graphite and gold[22] and demonstrates the capability of ITTC substrates for interacting with redox centres in the biofilm network allowing the transport of electrons from the cell interior to the electrode.[23-25]

Biofilms developed on ITTC were also evaluated by SEM (Fig. 2). The formation of thin biofilms was revealed, as previously observed on other porous electrodes;[10] suggesting that using macroporous substrates prevents somehow biomass development in excess, thus avoiding the accumulation of idle cells in upper layers of biofilms and consequently making the energy conversion process much more efficient. Confluent biofilms were observed totally covering both outer and inner aspects of the material, as expected from the implementation of a flow-through configuration. The large extent of colonization inside the conducting scaffold (Fig. 2C-E) gives support to the reported current yield and suggests that the macroporous ordered microstructure allows for a sufficient medium exchange to warrant biofilm growth.

In spite of the excellent performance of ITTC/Geobacter bioelectrodes, it is thought to be limited by an internal potential drop inside the porous scaffold, originated in the non-ideal distribution of current, known to occur along conducting lamellar configurations.[26] A manifestation of this effect is the wide potential window for total aperture of the redox signal controlling current evolution, which according to results in Fig. 2B expands from about -0.45 to 0.10 V. This limitation warrants further research in tunning for example, the pore size of these new electrodes to improve current density evolution, a task that can be easily performed by changing the cryogenic liquid (cooling temperature) in the ISISA method.

Conclusions

Whereas most of the efforts being made nowadays to increase anode performance in bioelectrochemical systems (BES) are focused on carbonaceous electrodes, in this study we demonstrate that ceramic materials can be an interesting alternative. In this study we combined the versatile chemistry of electrically conducting ceramics (Magnéli phases) with a cryogenic structuring technique (ISISA) to build up new macroporous 3D electrodes, termed ITTC (ice-templated titanium-based ceramic) electrodes.

The ITTC electrodes were shown to be biocompatible towards *G. sulfurreducens* while providing, at the same time, electrically conducting supports for the bacterial catalysis of acetate electro-oxidation. Their hierarchical structure offers an extremely large and reactive surface, outperforming virtually all carbonaceous materials described until present, when used as an anode in

View Article Online
DOI: 10.1039/C5EE01498K

bioelectrochemical reactors. Importantly, ITTC/Geobacter bioelectrodes provide higher volumetric current densities (as well as projected current densities and power densities) than those claimed as the target to support application developments,[20] finding a place in bio-energy production scaffolding as a real alternative in the area of microbial electrocatalysis (MEC). If we contribute to this insight, the goal of the present study will be accomplished.

Experimental

ITTC electrodes were prepared from TiO_2 aqueous dispersions *via* ice-segregation induced self-assembly (ISISA), followed by a high-temperature reducing process.

Preparation of TiO_2 dispersions. Dispersions were prepared by first dissolving 9.3 g of polyvinylpirrolidone (PVP, Aldrich, ~1.3MDa) in 150 mL of distilled water. Then, 31.5 g of TiO_2 nanoparticles (Degussa P25), ranging 20-30 nm in diameter, were added to the resulting solution and dispersed by means of a T25 Ultra-Turrax instrument at 25000 rpm. Thus-prepared TiO_2 dispersions exhibited long time stability (over 24 h) which represented a suitable time for processing the samples with no sedimentation or precipitation during this period.

ISISA of TiO_2 dispersions. TiO_2 porous scaffolds were prepared by directional freezing according to previously reported experimental conditions.[27] Briefly, the prepared TiO_2 aqueous dispersions (10 mL) were poured into plastic syringes (8 cm in length, 1.3 cm in diameter) and vertically dipped at a constant advancing ice front rate (5 mm/min) into a cold bath (liquid nitrogen, -196ºC). Immersions were performed at room pressure. The unidirectionally frozen samples were freeze-dried for 48 h (100 mtorr, -45ºC) using a VirTis Benchtop SLC (2KBTES-SS) freeze-drier. The obtained ultra-lightweight monoliths retained both the shape and size of the employed molds. For further treatments, the obtained porous cylinders were cut into samples of 2.5 cm in length.

ITTC electrode preparation. The freeze-dried TiO_2 porous scaffolds were used as precursors for preparing ITTC electrodes. For this, TiO_2 supports were first heat-treated at 1000°C for 1.5 h (heating and cooling rates of 5°C.min^{-1}) for sintering in an air atmosphere. This stage allowed mechanically consolidating the ceramic pieces. For this purpose, an electric furnace (Indef 332) was used. Electrically conducting Ti_4O_7 scaffolds were obtained from sintered TiO_2 porous monoliths after a high-temperature reducing process with elemental Zr, according to the following reaction:[18]

$$8\ TiO_2 + Zr \longrightarrow 2\ Ti_4O_7 + ZrO_2$$

15 mg of Zr per 100 mg of TiO_2 were used to obtain Ti_4O_7 Magnéli phase. The amount of Zr used corresponded to a 5% excess with respect to the stoichiometry of the reaction, as a requirement to obtain single phase Ti_4O_7 (see Fig.S1 in the Supplementary Material for the XRD characterization).[18] This phase displayed an electrical conductivity as high as that of graphite (see the electrical characterization of ITTC in the Supplementary Material – Fig.S2). To accomplish this, TiO_2 sintered samples (2 cm in length, 1 cm in diameter) were placed inside SiO_2-glass tubes separated by approximately 5 mm from Zr turnings (99% purity). The tubes were sealed under vacuum and subsequently heat-treated at 1000ºC (Indef 332 furnace) for 15 h, with heating and cooling rates of 5ºC/min.

Taking into consideration the overall process to obtain ITTC electrodes (from the TiO_2 aqueous dispersions to the finally reduced ITTC), an estimation of the manufacturing costs has been made. In our case, a lab-bench electrode was developed so it has to be taken into account that costs involved in each producing stage are not the lowest ones that could be found in the market. According to our estimate (on the material prices and processing considerations), a total cost of about US$ 7 per electrode was calculated (see calculation details in the Supplementary Material – Economic considerations on the ITTC electrode manufacturing). It is to be remarked that the same calculations, but only relying on material costs (not considering the processing stages – as sometimes reported),[32] led to a value of about US$ 0.28. This means that almost all the final electrode price relies on processing considerations, which should be taken into account when costs are reported.

Bacterial strain and culture medium. *Geobacter sulfurreducens* strain (DM12127, DSMZ, Germany) was used as a source of electrochemically active bacteria. The strain was anaerobically grown in stationary batch at 32ºC in an aqueous culture medium containing 30 mM KCl, 50 mM $NaHCO_3$, 9.3 mM NH_4Cl, 2.5 mM NaH_2PO_4, vitamins and trace minerals, according to previous protocols.[3,28] Prior to inoculation in the electrochemical cell, bacteria were cultured for three weeks in fumarate-containing (40 mM) growth medium (fumarate acting as electron acceptor) supplied with acetate (20 mM) used as carbon ource (electron donor).

Biofilm formation and ITTC electrode cell assembly under a flow-through configuration. ITTC electrodes were set in an electrochemical cell containing 100 mL deoxygenated culture medium lacking of any electron acceptor, and polarized at a constant potential of 0.2 V vs. Ag/AgCl (3M NaCl) reference electrode. Electrical contact to the external circuit was performed by gluing graphite rods on the conducting monoliths, using conducting epoxy adhesive. Graphite rods were prevented from contacting the liquid culture medium. To continuously supply fresh culture medium through the oriented macrochannels, the graphite bar (employed to make the external electrical contact) was hollowed with a drill and a rubber hose (1.5 mm in internal diameter) was placed in it. A peristaltic pump was used to inject culture medium (free of electron acceptors/free of planktonic cells) to the working cell, passing first through the porous electrode at a rate of 0.6 mL/min. The reactor and all liquid reservoirs were continuously flushed with a N_2:CO_2 mixture (80:20) to adjut the pH to 7.4 and to prevent oxygen contamination. Finally, 5 mL of stationary batch culture medium were inoculated through the working electrode to allow for bacterial growth and proliferation in the whole volume of the polarized porous platform. The electrochemical cell and culture medium were maintained at 32ºC under continuous stirring.

Characterization. Monolithic TiO_2 and ITTC structural

View Article Online
DOI: 10.1039/C5EE01498K

characteristics were assessed by scanning electron microscopy (**SEM**) on metalized samples by means of a Jeol JSM-6460 LV instrument. The same microscope was used to evaluate bacterial proliferation on the conducting scaffolds. For this purpose, bacteria adsorbed on monolith surfaces were first fixed in 2.5% glutaraldehyde during 60 min and then dehydrated during 10 min in alcoholic solutions (20, 40, 60, 80 and 100% ethanol). Samples thus prepared were air-dried, sectioned and metalized for SEM observations.

Bulk **densities** of the ceramic scaffolds (sintered and reduced bodies´ densities) were calculated from the weight and volume determined from precisely measured dimensions of each specimen. The porosity of each sample (%) was calculated as:

$$[1 - (\delta_c/\delta_r)] \times 100$$

where δ_c and δ_r are the calculated and the reported (rutile TiO_2[19] or Magnéli Ti_4O_7[18]) densities, respectively.

Electrochemical assays were performed in an electrochemical cell using graphite rods (control) or ITTC as working electrodes, polarized at a constant potential of 0.2 V vs. Ag/AgCl (3M NaCl) reference electrode and using a platinum wire as a counter-electrode. Tests were performed using a PGSTAT 101 potentiostat, controlled by the NOVA 1.6 software. Cyclic voltammetries were conducted by scanning a -0.6 V/0.6 V potential range, using a scanning rate of 0.01 V/s. The production of current was followed in time by chronoamperometry, acquiring 1 point per minute. All presented results are representative of those obtained from at least three independent tests conducted under the same experimental conditions.

Acknowledgements

This work was supported by the National Research Council (CONICET, Argentina), the National Agency for the Promotion of Science and Technology (ANPCyT, Argentina) and the Argentinean Nanotechnology Foundation (FAN).

Supplementary Information

- Powder X-ray diffraction (XRD) characterization of the Ti_4O_7 electrode material (Fig.S1).
- Electrical characterization of ITTC compared to a typical carbon electrode (Fig.S2).
- Chronoamperometric comparison between ITTC electrode, Ti_4O_7 dense electrode and a typical graphite bar (Fig.S3).
- SEM characterization of *G. sulfurreducens* biofilm grown on Ti_4O_7 dense electrodes (Fig.S4).
- Cyclic voltammetry tests on the ITTC electrode during *G. sulfurreducens* biofilm evolution (Fig.S5).
- Cyclic voltammetry tests after *G. sulfurreducens* biofilm formation on ITTC and a typical graphite bar (Fig.S6).
- Protocol for the preparation of Ti_4O_7 dense electrodes and SEM characterization of *G. sulfurreducens* biofilms grown on dense Ti_4O_7.
- Economic considerations on the ITTC electrode manufacturing.

Notes and references

[a] *Laboratorio de Bioelectroquímica, Instituto de Investigaciones en Ciencia y Tecnología de Materiales (INTEMA), Consejo Nacional de Investigaciones Científicas y Técnicas (CONICET), 7600, Mar del Plata, Argentina.*
[b] *División Cerámicos, Instituto de Investigaciones en Ciencia y Tecnología de Materiales (INTEMA), Consejo Nacional de Investigaciones Científicas y Técnicas (CONICET), 7600, Mar del Plata, Argentina.*
[c] *División Polímeros Nanoestructurados, Instituto de Investigaciones en Ciencia y Tecnología de Materiales (INTEMA), Consejo Nacional de Investigaciones Científicas y Técnicas (CONICET), 7600, Mar del Plata, Argentina. E-mail: hromeo@fi.mdp.edu.ar*

1. D. R. Lovley and K. P. Nevin, *Curr. Opin. Biotech.*, 2011, **22**, 1.
2. B. E. Logan and K. Rabaey, *Science*, 2012, **337**, 686.
3. G. D. Schrott, M. V. Ordoñez, L. Robuschi and J. P. Busalmen, *ChemSusChem*, 2013, n/a-n/a.
4. K. P. Nevin, H. Richter, S. F. Covalla, J. P. Johnson, T. L. Woodard, A. L. Orloff, H. Jia, M. Zhang, D. R. Lovley, *Environ. Microbiol.*, 2008, **10**, 2505.
5. P. S. Bonanni, D. F. Bradley, G. D. Schrott and J. P. Busalmen, *ChemSusChem*, 2013, **6**, 711-720.
6. L. Robuschi, J. P. Tomba, G. D. Schrott, P. S. Bonanni, P. M. Desimone and J. P. Busalmen, *Angewandte Chemie*, 2013, **52**, 925-928.
7. S. Chen, G. He, X. Hu, M. Xie, S. Wang, D. Zeng, H. Hou and U. Schröder, *ChemSusChem*, 2012, **5**, 1059.
8. S. Chen, Q. Liu, G. He, Y. Zhou, M. Hanif, X. Peng, S. Wang and H. Hou, *J. Mater. Chem.* 2012, **22**, 18609.
9. S. Chen, G. He, Q. Liu, F. Harnisch, Y. Zhou, Y. Chen, M. Hanif, S. Wang, X. Peng, H. Hou and U. Schröder, *Energy Environ. Sci.*, 2012, **5**, 9769-9772.
10. V. Flexer, J. Chen, B. C. Donose, P. C. Sherrell and G. G. Wallace, *Energy Environ. Sci.*, 2013, **6**, 1291.
11. S. Chen, H. Hou, F. Harnisch, S. A. Patil, A. A. Carmona-Martinez, S. Agarwal, Y. Zhang, S. Sinha-Ray, A. L. Yarin, A. Greiner and U. Schröder, *Energy Environ. Science*, 2011, **4**, 1417-1421.
12. K. Katuri, M. L. Ferrer, M. C. Gutierrez, R. Jimenez, F. Del Monte and D. Leech, *Energy Environ. Science*, 2011, **4**, 4201-4210.
13. A. Fujishima and X. C. Zhang, *R. Chim.*, 2005, **9**, 750.
14. B. O´Regan and M. Gratzel, *Nature*, 1991, **353**, 737.
15. M. Canillas, E. Chinarro, M. Carballo-Vila, J. R. Jurao and B. Moreno, *J. Mater Chem.. B*, 2013, **1**, 6459.
16. H. Romeo, F. Trabadelo, M. Jobbágy and R. Parra, *J. Mater. Chem. C*, 2014, **2**, 2806.
17. J. R. Smith, F. C. Walsh and R. L. Clarke, *J. Appl. Electrochem.*, 1998, **28**, 1021.
18. A. Kitada, G. Hasegawa, Y. Kobayashi, K. Kanamori, K. Nakanishi and H. Kageyama, *J. Am. Chem. Soc.*, 2012, **134**, 10894.
19. U. Diebold, *Surf. Sci. Rep.*, 2003, **48**, 53.
20. V. Eyert, U. Schwingenschlögl and U. Eckern, *Chem. Phys. Lett.*, 2004, **390**, 151.
21. A. P. Borole, G. Reguera, B. Ringeisen, Z-W. Wang, Y. Feeng, B. H. Kim, *Energy Environ. Science*, 2011, **4**, 4813-4834.
22. B. Maestro, J. M. Ortiz, G. Schrott, J. P. Busalmen, V. Climent and J. M. Feliu, *Bioelectrochemistry*, 2014, **98**, 11.
23. E. Marsili, J. B. Rollefson, D. B. Baron, R. M. Hozalski and D. R. Bond, *Appl. Environ. Microbiol.*, 2008, **74**, 7329.
24. J. P. Busalmen, A. Esteve-Núñez, A. Berná and J. M. Feliu, *Angew. Chem. Int. Ed.*, 2008, **47**, 4874.
25. H. Richter, K. P. Nevin, H. Jia, D. A. Lowy and D. R. Lovley, *Energy Environ. Sci.*, 2009, **2**, 506.
26. R. Lacroix, S. Da Silva, M. V. Gaig, R. Rousseau, M. L. Délia and A. Bergel, *Phys. Chem. Chem. Phys.*, 2014, **16**, 22892.
27. H. E. Romeo, C. E. Hoppe, M. A. López-Quintela, R. J. J. Williams, Y. Minaberry and M. Jobbágy, *J. Mat. Chem.*, 2012, **22**, 9195.
28. A. Esteve-Núñez, M. Rothermich, M. Sharma and D. Lovley, *Environ. Microbiol.*, 2005, **7**, 641.

View Article Online
DOI: 10.1039/C5EE01498K

29. M. Sharma, S. Bajracharya, S. Gildemyn, S.A. Patil, Y. Alvarez-Gallego, D. Pant, K. Rabaey and X. Dominguez-Benetton, *Electrochimica Acta* 2014, **140**, 191.
30. X. Xie, L.Hu, M. Pasta, G.F. Wells, D. Kong, C. S. Criddle and Y.Cui, *Nano Lett.* 2011,**11**, 291.
31. Y. Liu, F. Harnish, K. Fricke, U. Schröder, V. Climent and J. M. Feliu, *Biosens. Bioelectron.*, 2010, **25**, 2167.
32. A. Baudler, I. Schmidt, M. Langner, A. Greiner, U. Schroder, *Energy Environ. Sci.* 2015, DOI: 10.1039/C5EE00866B